Particle-In-Cell Simulations of 100 keV Electron Beam Interaction with a Thin Magnetized Plasma

Annenkov V. V.[1,2,a)], Timofeev I.V.[1,2] and Volchok E.P.[1,2]

[1]*Budker Institute of Nuclear Physics, Siberian Branch of Russian Academy of Sciences, Novosibirsk, Russia.*
[2]*Novosibirsk State University, Novosibirsk, Russia.*

[a)]Corresponding author: annenkov.phys@gmail.com

Abstract. First simulation results on interaction of a long and thin magnetized plasma column with a 100 keV electron beam are presented. Selected parameters are similar to those in the real GOL-3 experiments. To simulate the realistic problem of continuous beam injection into a plasma, we use a 2D3V particle-in cell code allowing for the open boundary conditions in the beam direction. It is shown that such a thin system appears to be unstable against the quasi-regular longitudinal density modulations and generates the fundamental and second harmonic emissions via the antenna mechanism. The radiation power of such an antenna is found to reach 0.6% of the total beam power.

INTRODUCTION

Collective interactions of powerful electron beams with magnetized plasmas have long been studied both theoretically and experimentally. At the multi-mirror trap GOL-3 (BINP SB RAS, Novosibirsk), recent laboratory experiments have demonstrated the regime at which 1% of the beam power is converted to the power of electromagnetic emission. The main pecularity of this regime is that a 100 keV electron beam creates a thin plasma column with the diameter comparable to the radiation wavelength[1]. Theoretical studies[2, 3, 4] motivated by these experiments have shown that such a high level of radiation efficiency can be explained by the mechanism of beam-plasma antenna. This theory is based on the fact that, in a thin plasma with a longitudinal density modulation, the beam-excited mode can generate the superluminal satellite which can resonate with vacuum electromagnetic waves. The required density profile can appear self-consistently under the influence of a modulational instability pumping by the dominant beam-driven wave.

In this paper, we consider beam-plasma parameters which are similar to the experimental regime with 1% emission efficiency. We use a mildly-relativistic beam with the mean velocity $v_{beam} = 0.548c$. The beam and plasma have Maxwellian momentum distributions $f^{(e,b)} \propto \exp(-\mathbf{p}^2/2\Delta p^2_{(e,b)})$ with corresponding temperatures $T_{(e,b)} = \Delta p^2_{(e,b)}/2m_e$. In our simulations ions are initially cold. Such an ion temperature is typical to the GOL-3 experiments where plasma electrons are heated much faster than plasma ions. The plasma column has the sizes $L_y \times L_x = 6mm \times 30cm$. Other simulation parameters are presented in Table 1. To construct a system with open boundaries in the x direction, we use special buffers in which the initial distributions of plasma particles are continuously supported. The plasma column is separated from the boundaries by vacuum regions with the characteristic width of $403h$. Near the boundaries of the simulation box, we construct the damping layers in which the electromagnetic fields are artificially absorbed.

TABLE 1. System parameters

Simulation box size	4520×1136 cells	Plasma density	$10^{13} cm^{-3}$
Grid step	$h = 0.04c/\omega_p$	Current density	$300\, A/cm^2$
Time step	$\Delta t = 0.02\omega_p^{-1}$	External magnetic field	$B_x = 1.24\, T$
Number of particles	$N_p \approx 68 \cdot 10^6$	Beam and electron temperature	$150\, eV$ and $80\, eV$
Plasma frequency	$\omega_p = 1.78 \cdot 10^{11}\ s^{-1}$	Electron cyclotron frequency	$\Omega_e = 1.22\omega_p$

RESULTS OF SIMULATIONS

We simulate the beam injection during the time period 7.5 ns. Despite the large length of the system (30 cm), all significant processes are localized in a small spatial region near the injector ($z < 5$ cm). It is caused by the strong beam-plasma instability that results in the formation of the quasi-one-dimensional high amplitude wave packet with the length 3 cm by the moment 1 ns from the start of injection (Fig.2a). In this packet, the wave energy is nonlinearly saturated by beam trapping and the beam distributuion extends down to zero velocities (Fig.2c). Under the field of such an energetic wave, a modulational instability develops.

Let us now study these processes in details. According to the linear theory an electron beam in a plasma drives a wave with the frequency $\omega_b = \omega_p(1 - \widehat{n}_b^{1/3}/(2^{4/3}\gamma_b))$, where $\widehat{n}_b$ is the beam density in units of plasma density, γ_b – beam relativistic factor, ω_p – plasma frequency. For our parameters the frequency and wavenumber (in units of ω_p/c) of this dominant mode should equal to $\omega_b = 0.925\omega_p$ and $k_\parallel = 1.7$. In our simulations, however, the spectrum of resonant waves is not represented by a single mode, but occupies the relatively wide region in the wavenumber space (Fig. 1a) with the slightly shifted dominant frequency $\omega_b \approx 0.87\omega_p$. This indicates about the significant role of nonlinear effects. Development of the modulation instability leads to the growth of small-scale ion density fluctuations with wavenumbers $q = 9.2$ and $q = 5.4$ (Fig. 1a) responsible for the subsequent plasma heating by the time moment $t = 140\omega_p^{-1}$. Simultaneously, we observe the directional EM radiations (Fig. 2a, b) near the plasma frequency and its second harmonic (Fig. 2d). Origin of these radiations can be explained in terms of the beam-plasma antenna theory. Density fluctuations upon which scattering of primary plasma waves creates superluminal waves of electric current are shown in (Fig. 1a). It is seen that the density peak with $q = 6.4$ can generate only $2\omega_b$ emission due to the nonlinear coupling of the dominant beam-driven mode $(\omega_b, k_\parallel)$ with its long-wavelength satellite $(\omega_b, k_\parallel - q)$. Generation near ω_b should be more efficient than near $2\omega_b$, , but the second harmonic radiation dominates due to much lower density perturbations with small q at this stage.

Modulation instability conditions are quickly changed with the increase of plasma temperature. Thereby, by the moment $t = 716\omega_p^{-1}$, small-scale ion density perturbations with high q decay. Contrary, the small q spectrum begins to grow (Fig. 1b). We can distinguish two main peaks in the spectra of beam-driven waves. The first one ($k_\parallel = 1.7$) corresponds to the primary traveling wave and the second ($k_\parallel = 2.2$)(also visible in the ion density spectrum) relates to the modulational perturbations. The nonlinear stage of the modulational instability is accompanied by trapping of beam-driven waves into corresponding density wells, that is why, in Fig.3c, one can see the standing plasma oscillations. The wavelength of these trapped oscillations is automatically adjusted to the modulation length ($k_\parallel = 2.2 = q$), which allows the plasma antenna to radiate more efficiently in the transverse direction at the frequency ω_b. Figure 3d also shows that ω_b- and $2\omega_b$-radiations are characterized by equal intensities, but strongly separated over polarizations.

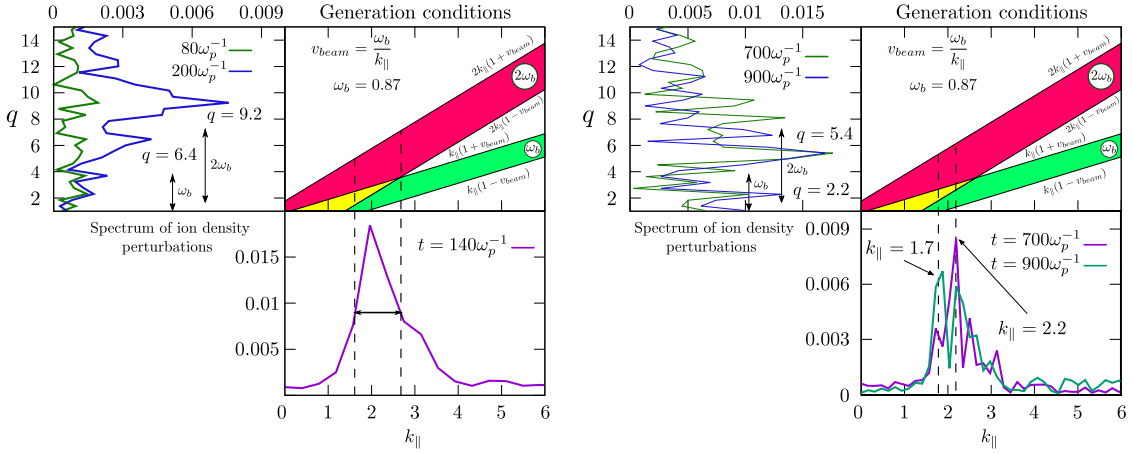

a) Time moment near $140\omega_p^{-1}$

b) Time moment near $716\omega_p^{-1}$

FIGURE 1. In both subfigures: top left – ion density spectra in different times; bottom right – spectra of the plasma wave in the center of the plasma layer; top right – conditions for the antenna emissions. Green area corresponds to radiation near the plasma frequency, red – to the second harmonic, yellow – to their intersection.

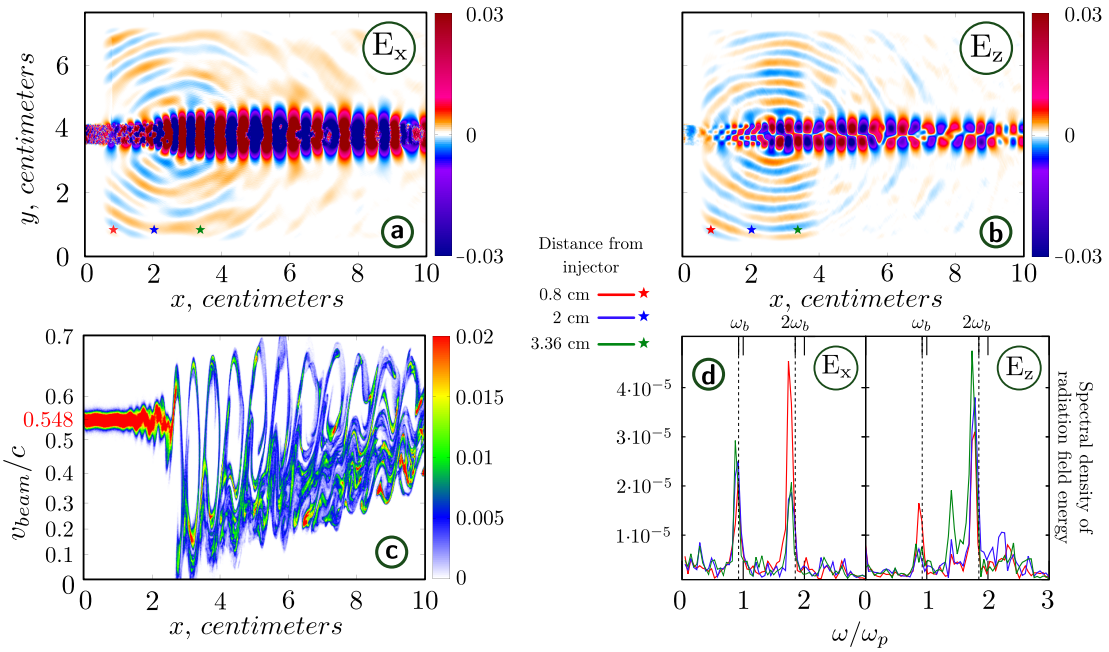

FIGURE 2. Time moment near $140\omega_p^{-1}$ (0.8 ns from the start of injection). (a) and (b) The maps of electric fields E_x and E_z. Points of frequency spectra measuring (stars) (c) The phase space $(x; v_x)$ of beam electrons. (d) The frequency spectra of E_x and E_z measured in the single points lying near the damping layer (red, blue and green stars).

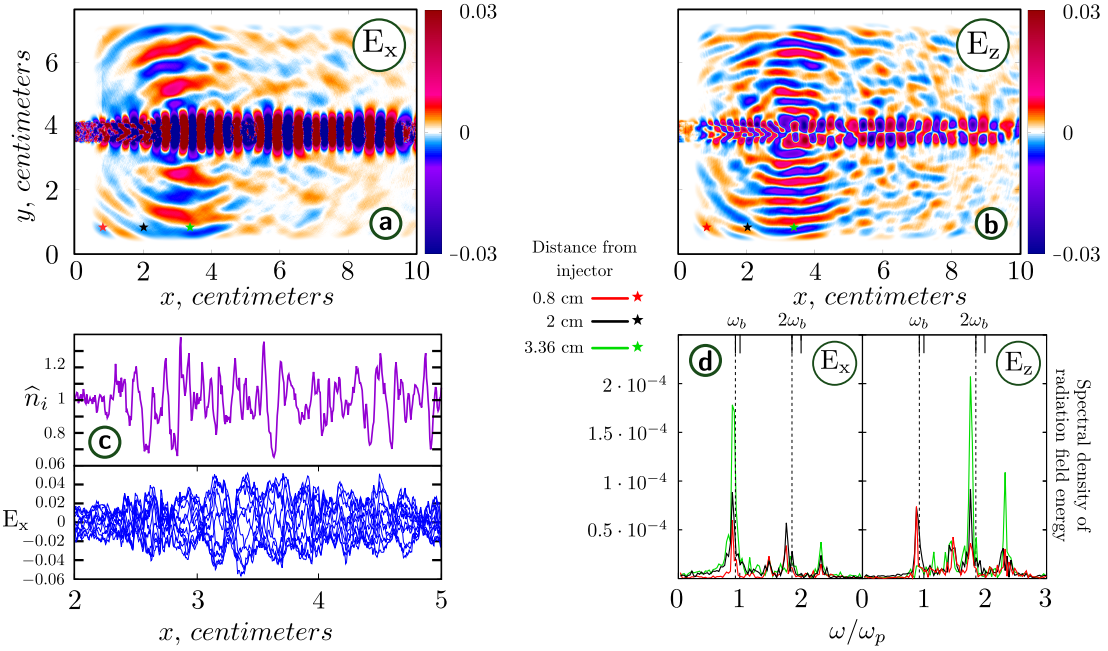

FIGURE 3. Time moment near $716\omega_p^{-1}$ (4 ns from the start of injection). (a) and (b) The maps of electric fields E_x and E_z. Points of frequency spectra measuring (stars) (c) Electric fields E_x in the center of the plasma layer and corresponding y-averaged density profiles (multiple curves for E_x correspond to the different phases of a single plasma oscillation). (d) The frequency spectra of E_x and E_z measured in the single points lying near the damping layer (red, black and green stars).

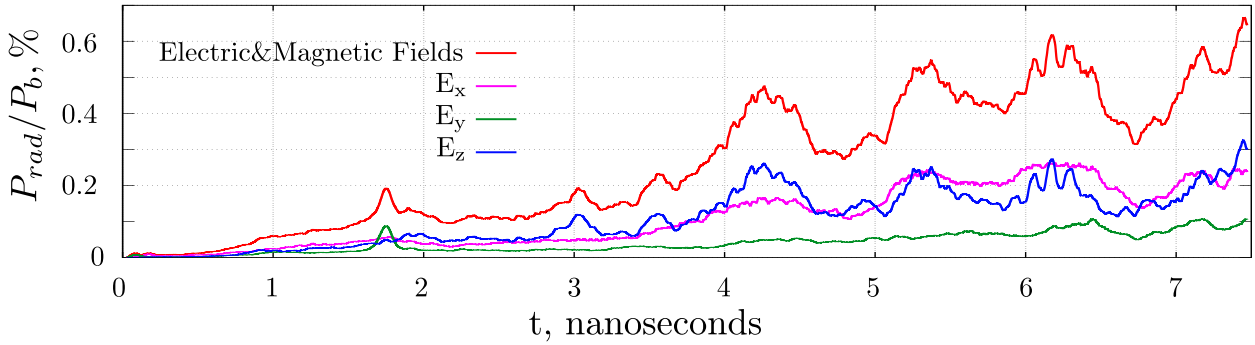

FIGURE 4. The total power of both fundamental and harmonic emissions, which is absorbed in all damping layers near the boundaries of the simulation box.

The temporal dependence of radiation efficiency defined as the ratio of emission power to the beam power is presented in Fig.4. After the development of modulational instability, it demonstrates a periodic structure with the 1 ns time-scale. Such periodic fluctuations are associated with a cyclic process of trapping and consequent burning out of standing plasma oscillations inside the corresponding density wells. Since ω_b- and $2\omega_b$-radiations are characterized by E_x-and E_z-polarizations, we can conclude that their intensities are always comparable. The total power of EM radiation reaches 0.6% of beam power.

SUMMARY AND DISCUSSION

For the first time, relaxation of a mildly-relativistic electron beam in a hot magnetized plasma and subsequent EM emission processes are studied by the particle-in-cell numerical code allowing for the continuous beam injection at scales and parameters typical to real laboratory experiments. Dynamics of EM radiations near the plasma frequency and its second harmonic is well explained by the antenna mechanism which provides the high emission efficiency 0.6% in a good agreement with experimental results. Simulations show, however, that the intense radiation is localized inside the region of several centimeters which does not agree with experimental data. The reason for that is possibly explained by the fact that we do not take into account regular gradients of plasma density capable of stabilizing the beam-plasma instability at the entry to the magnetic trap. On the other hand, the radiating region can be removed away from the injector by changing of system parameters at later times. Verification of these possibilities needs further investigations.

ACKNOWLEDGMENTS

This work is supported by the Russian Foundation for Basic Research (grant 15-32-20432).

REFERENCES

[1] A. Burdakov *et al.*, Fusion Sci. Technol. **63**, 286–288 (2013).
[2] I. V. Timofeev, V. V. Annenkov, and A. V. Arzhannikov, Phys. Plasmas **22**, p. 113109 (2015).
[3] V. Annenkov, E. Volchok, and I. Timofeev, Plasma Phys. Controlled Fusion **58**, p. 045009 (2016).
[4] V. Annenkov, I. Timofeev, and E. Volchok, Phys. Plasmas **23**, p. 053101 (2016).